Stem Cell Research 34 (2019) 101357

Contents lists available at ScienceDirect

Stem Cell Research

journal homepage: www.elsevier.com/locate/scr

Lab Resource: Multiple Cell Lines

Generation of two induced pluripotent stem cell lines from a patient with dominant *PRPF31* mutation and a related non-penetrant carrier

Samuel McLenachan[a,b,1], Dan Zhang[b,1], Xiao Zhang[a], Shang-Chih Chen[b], Tina Lamey[a,c], Jennifer A. Thompson[c], Terri McLaren[c], John N. De Roach[a,c], Sue Fletcher[e], Fred K. Chen[a,b,c,d,*]

[a] *Centre for Ophthalmology and Visual Science, The University of Western Australia, Nedlands, Western Australia, Australia*
[b] *Lions Eye Institute, Nedlands, Western Australia, Australia*
[c] *Australian Inherited Retinal Disease Registry and DNA Bank, Department of Medical Technology and Physics, Sir Charles Gairdner Hospital, Nedlands, Western Australia, Australia*
[d] *Department of Ophthalmology, Royal Perth Hospital, Perth, Western Australia, Australia*
[e] *Centre for Comparative Genomics, Murdoch University, Western Australia, Australia*

A B S T R A C T

We report the generation of the human iPSC line LEIi008-A from a patient with retinitis pigmentosa-11 caused by a dominant nonsense mutation in the *PRPF31* gene (NM_015629.3:c.1205C > A p.(Ser402Ter)). A second line, LEIi009-A, was generated from a related non-penetrant carrier of the same mutation with no retinal disease. Reprogramming of patient dermal fibroblasts using episomal plasmids containing *OCT4*, *SOX2*, *KLF4*, *L-MYC*, *LIN28*, shRNA for *p53* and mir302/367 microRNA generated cell lines displaying pluripotent stem cell marker expression, a normal karyotype and the capability to differentiate into the three germ layer lineages.

Resource table

Unique stem cell lines identifier	LEIi008-A LEIi009-A
Alternative names of stem cell lines	1093ips4 (LEIi008-A) 1374ips1 (LEIi009-A)
Institution	Lions Eye Institute, Nedlands, Western Australia, Australia
Contact information of distributor	Samuel McLenachan: smclenachan@lei.org.au Fred Chen: fredchen@lei.org.au
Type of cell lines	iPSC
Origin	Human
Cell Source	Dermal fibroblasts
Clonality	Clonal
Method of reprogramming	Episomal
Multiline rationale	Unaffected mother and affected son carrying same dominant *PRPF31* mutation
Gene modification	Yes
Type of modification	Hereditary
Associated disease	Retinitis Pigmentosa 11
Gene/locus	*PRPF31*/19q13.42
Method of modification	N/A
Name of transgene or resistance	N/A
Inducible/constitutive system	N/A
Date archived/stock date	LEIi008-A: 18/12/17; LEIi009-A: 17/11/17
Cell line repository/bank	https://hpscreg.eu/cell-line/LEIi008-A https://hpscreg.eu/cell-line/LEIi009-A
Ethical approval	Human Research Ethics Office, University of Western Australia (RA/4/1/7916)

* Corresponding author at: The Lions Eye Institute, 2 Verdun Street, Nedlands, Western Australia 6009, Australia.
E-mail address: fredchen@lei.org.au (F.K. Chen).
[1] These authors contributed equally.

https://doi.org/10.1016/j.scr.2018.11.018
Received 28 October 2018; Received in revised form 23 November 2018; Accepted 27 November 2018
Available online 10 December 2018

Resource utility

Retinitis pigmentosa-11 (RP11) is caused by dominant mutations in the *PRPF31* gene, however up to 30% of *PRPF31* mutation carriers are non-penetrant. The two iPSC lines described here were derived from an RP11 patient and his unaffected mother and provide a unique opportunity to examine the non-penetrance of RP11 mutations.

Resource details

RP11 is the most common form of autosomal dominant retinitis pigmentosa and is caused by dominant mutations in the *PRPF31* gene, which encodes the pre-RNA processing factor-31 protein. Despite the ubiquitous expression of *PRPF31*, mutations in this gene specifically affect the retina, leading to visual impairment and retinal degeneration. The pathophysiology of RP11 is thought to be driven by *PRPF31* haploinsufficiency (Rose and Bhattacharya, 2016), with retinal tissues preferentially affected due to their high dependence on alternative splicing (Wilkie et al., 2006). Reduced levels of total *PRPF31* transcript as well as a delayed rate of spliceosome assembly and pre-mRNA processing have been reported in RP11 patients (Frio et al., 2008). Interestingly, RP11 displays non-penetrance in affected families, with 30% of carriers remaining free from retinal disease. The non-penetrance of *PRPF31* mutations has been associated with modifying factors influencing expression of the unaffected *PRPF31* allele, such as promoter elements and transcriptional repressors (Rose and Bhattacharya, 2016).

We identified an Indigenous Australian family affected by RP11. Affected individuals displayed posterior subcapsular cataract, rod cone dystrophy and macular cysts with onset of symptoms ranging from 5 to 25 years of age. All affected siblings ($n = 4$) carried the NM_015629.3:c.1205C > A p.(Ser402Ter) mutation. Dermal fibroblasts were cultured from skin biopsies taken from an affected RP11 patient and his unaffected mother, both of whom carried the c.1205C > A mutation in *PRPF31*. The presence of the c.1205C > A mutation in each fibroblast line was confirmed Sanger sequencing of a PCR product (Fig. 1A). Fibroblasts from each patient were transfected with episomal plasmids containing *OCT4*, *SOX2*, *KLF4*, *L-MYC*, *LIN28*, shRNA for *p53* and mir302/367 microRNA. After 20–25 days, colonies were picked for clonal expansion. LEIi008-A iPSC were derived from the affected male patient, while LEIi009-A iPSC were derived from his unaffected mother (Table 1, Table 2). Both lines displayed morphology typical of pluripotent stem cell cultures (Fig. 1A). DNA fingerprinting by short tandem repeat analysis demonstrated each iPSC line matched its donor fibroblast line at 16 loci (Supplementary Fig. S1). Expression of the OCT4, NANOG and SOX2 proteins as well as the pluripotency marker TRA-1-81 was demonstrated in both lines by immunocytochemistry (Fig. 1B). Digital karyotyping by genome-wide SNP profiling and copy number variation analysis demonstrated LEIi008-A nor LEIi009-A had undergone genomic alterations, with both lines displaying a normal karyotype (46,XY and 46,XX, respectively, Fig. 1C, Supplementary Fig. S2). Quantitative RT-PCR demonstrated both LEIi008-A and LEIi009-A expressed similar levels of pluripotency marker expression to a commercial control human iPSC line (Fig. 1D). PCR screening demonstrated both lines were negative for mycoplasma and for episomal reprogramming plasmids (Supplementary Fig. S3). After two weeks of spontaneous differentiation, embryoid bodies derived from LEIi008-A and LEIi009-A expressed markers of ectoderm (*PAX6*, *OTX1*), mesoderm (*DCN*, *GATA2*) and endoderm (*AFP*) (Fig. 1E). To demonstrate the capacity for retinal differentiation, LEIi008-A and LEIi009-A were differentiated as retinal organoids. After 2 months, both lines produced retinal organoids containing pigmented RPE cells. RPE cells were isolated from retinal organoid cultures and cultured as pure monolayers (Fig. 1F, micrographs). After 3 weeks of differentiation, quantitative RT-PCR analysis demonstrated iPSC-RPE from both donors expressed the RPE markers *RPE65* and *BEST1* and downregulated *OCT4* expression (Fig. 1F, graph).

Materials and methods

Cell culture and reprogramming

Patient fibroblasts were cultured in DMEM medium supplemented with 10% fetal calf serum and antibiotic-antimycotic (ThermoFisher). Patient iPSCs were cultured in feeder-free conditions, on Geltrex-coated (ThermoFisher) culture plates in TeSR-E8 medium (StemCell Technologies). For passaging, iPSC were treated with EDTA Buffer (1xDPBS without Ca^{+2} and Mg^{+2}/0.5 mM EDTA/30 mM NaCl) for 5 min at room temperature. The buffer was then removed and replaced with TeSR-E8 media. Colonies were then mechanically scraped into the media and seeded into new Geltrex-coated culture wells at a ratio of 1:3–1:5. Media changes were performed daily and passaging was performed every 4–5 days. All cultures were maintained in a humidified incubator at 37 °C with 5% CO_2. Patient fibroblasts were reprogrammed using the Episomal iPSC Reprogramming Plasmid kit (SC900A-1, System Biosciences), according to the manufacturer's instructions. Colonies were picked for clonal expansion on days 21–25. PCR screening for episomal plasmids was performed at passage 9 for LEIi008-A and passage 10 for LEIi009-A, with fibroblasts transfected with reprogramming episomes and early passage iPSC used as positive controls. PCR was performed using SYBR PCR Master Mix (QIAGEN) and 200 nM of each primer. The reactions were performed on the CFX Connect Real-Time PCR Detection System (Biorad) using the following cycling conditions: 95 °C for 5 s, then 30 cycles of 95 °C for 10s and 60 °C for 15 s. Mycoplasma testing was performed using the Lookout Mycoplasma PCR Detection Kit (Sigma-Aldrich) according to the manufacturer's instructions. A commercial iPSC line (ThermoFisher, Cat#A18945, HuiPSC) was used as a control.

iPSC differentiation

For trilineage differentiation, iPSCs were cultured as embryoid bodies (EBs). IPSC were treated with EDTA Buffer for 5 min at room temperature, the buffer was then removed and replaced with TeSR-E8 media containing 10 μM Y27632 (Abcam). Colonies were mechanically scraped into the media, and then seeded into Greiner suspension culture 6 well plates in TeSR-E8 media supplemented with 10 μM Y27632. On day 3, the media was changed to DMEM/F12 supplemented with 20% knockout serum replacement (KSR), Minimal Essential Media Non-Essential Amino Acids Solution (NEAA) and antibiotic-antimycotic (ThermoFisher). Media was changed every second day. On day 14, EBs were collected for qPCR analysis. Trilineage differentiation was assessed by the induction of genes for ectoderm (*PAX6, OTX1*) endoderm (*AFP*) and mesoderm (*DCN, GATA2*). For directed differentiation into retinal organoids we followed a previously published protocol (Mellough et al., 2012). After 2 months of differentiation, organoids containing pigmented RPE were collected and treated with TrypLE™ Express Enzyme (ThermoFisher) for 10 min at 37 °C. The RPE cells were seeded into Geltrex-coated wells of a 24 well plate in RPE media (DMEM/F12, NEAA, B27, N2, 10 ng/ml IGF-1, 4% KSR and antibiotic-antimycotic).

qPCR analysis

Total mRNA was isolated using TRIzol Reagent (ThermoFisher) and cDNA was synthesized using the RT^2 First Strand Kit (Qiagen). qPCR reactions were prepared using RT^2 SYBR Green qPCR Mastermixes (Qiagen),

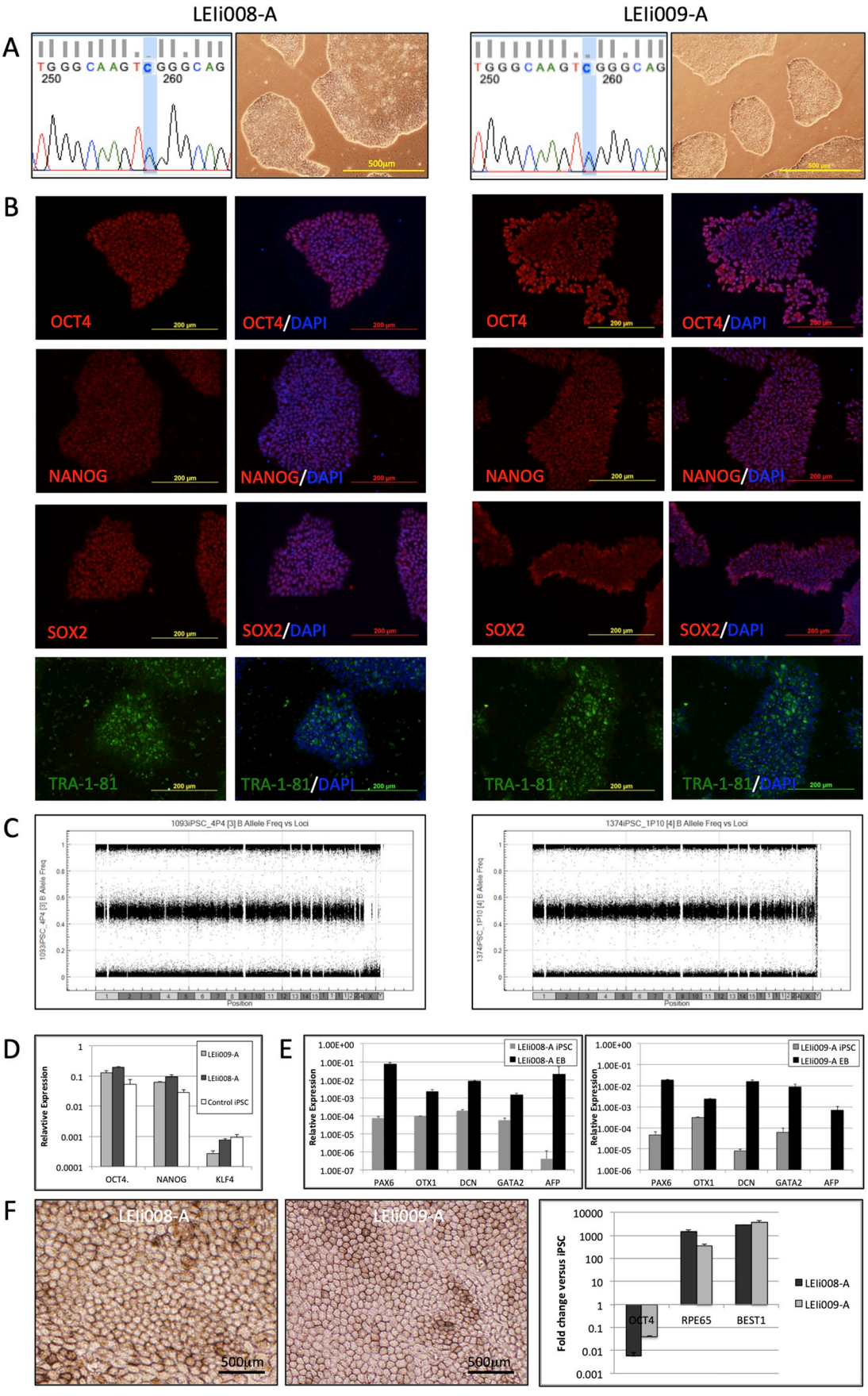

(caption on next page)

Fig. 1. A: Sanger sequencing of the PRPF31 gene demonstrated the presence of the c.1205C > A mutation in the parental fibroblasts used to generate the LEIi009-A and LEIi009-A iPSC lines (chromatograms). Both LEIi008-A and LEIi009-A displayed morphologies typical of pluripotent stem cell colonies (images). B: The expression of pluripotency markers (OCT4, NANOG, SOX2 and TRA-1-81) in LEIi008-A and LEIi009-A was demonstrated by immunocytochemistry. Nuclei were counterstained with DAPI (merged images). C: Digital karyotyping of LEIi008-A and LEIi009-A was performed using the Illumina HumanCoreExome-24 Beadchip SNP array. B-allele frequencies were plotted against genomic location for 500,000 human SNPs, demonstrating normal, 46,XY and 46,XX karyotypes in each line respectively. D: Quantitative RT-PCR demonstrated similar levels of expression of pluripotency genes (*OCT4*, *NANOG*, and *KLF4*) in LEIi008-A (grey bars) and LEIi009-A (dark grey bars) and a commercial human iPSC line (white bars). Relative expression values were normalised to *GAPDH* expression using the ΔCt method. Error bars indicate standard deviation. E: Expression of ectodermal (*PAX6*, *OTX1*), mesodermal (*DCN*, *GATA2*) and endodermal (*AFP*) genes was increased in embryoid bodies (black bars) derived from LEIi008-A (left graph) and LEIi009-A (right graph), compared with undifferentiated iPSC (grey bars). Relative expression values were normalised to *GAPDH* expression using the ΔCt method. Error bars indicate standard deviation. F: Monolayers of RPE cells could be derived from LEIi008-A (left image) and LEIi009-A (right image) iPSC. Quantitative PCR analysis demonstrated expression of the RPE markers *RPE65* and *BEST1* was upregulated in RPE derived from both patient iPSC lines, while expression of *OCT4* was downregulated. Expression values were calculated using the ΔΔCt method, normalised to *GAPDH* and expressed as fold changes compared with undifferentiated iPSC. Error bars indicate standard deviation.

Table 1
Summary of lines.

iPSC line names	Abbreviation in figures	Gender	Age	Ethnicity	Genotype of locus	Disease
LEIi008-A	1093IPSC_4P4	Male	28	Indigenous Australian	*PRPF31* c.1205C > A	RP11
LEIi009-A	1374IPSC_1P10	Female	54	Indigenous Australian	*PRPF31* c.1205C > A	RP11

Table 2
Characterization and validation.

Classification	Test	Result	Data
Morphology	Photography	Normal	Fig. 1 panel A
Phenotype	Qualitative analysis: Immunocytochemistry	Positive staining for pluripotency markers: OCT4, NANOG, SOX2, TRA-1-81	Fig. 1 panel B
	Quantitative analysis: RT-qPCR	Expression of *OCT4*, *NANOG* and *KLF4*	Fig. 1 panel D
Genotype	Digital Karyotyping by Illumina SNP Beadchip and CNV analysis	LEIi008-A: 46, XY LEIi009-A: 46, XX Resolution: 500 kB	Fig. 1 panel C, Supplementary Fig. S2
Identity	STR analysis	LEIi008-A: Matched at 16 loci LEIi009-A: Matched at 16 loci	Supplementary Fig. S1 Raw data available with the authors
Mutation analysis (IF APPLICABLE)	Sequencing	LEIi008-A *PRPF31* c.1205C > A (Heterozygous) LEIi009-A: *PRPF31* c.1205C > A (Heterozygous)	Fig. 1 panel A
Microbiology and virology	Mycoplasma	Mycoplasma testing by PCR: Negative	Supplementary Fig. S3B
Differentiation potential	Embryoid body formation	Induction of ectoderm (*PAX6*, *OTX1*), mesoderm (*DCN*, *GATA2*) and endoderm (*AFP*, *SOX7*) marker gene expression	Fig. 1 panel E
	Directed differentiation to retinal organoids	Induction of pigmented RPE cells expressing *RPE65* and *BEST1*	Fig. 1 panel F
Donor screening (Optional)	HIV 1 + 2 Hepatitis B, Hepatitis C	N/A	N/A
Genotype additional info (Optional)	Blood group genotyping	N/A	N/A
	HLA tissue typing	N/A	N/A

and performed using the CFX Connect Real-Time System (BioRad). Data was analyzed using the ΔΔCT method. Gene expression values were normalized to *GAPDH* expression. Primers used are listed in Table 3.

Immunostaining analysis

Cells were fixed with 4% paraformaldehyde for 15 min at 37 °C, washed, then permeabilized using phosphate buffered saline (PBS) with 0.3% Triton X-100 for 15 min. The cells were then incubated in blocking buffer (5% normal goat serum with 0.3% Triton X-100 (Sigma-Aldrich) in PBS) for 1 h at room temperature. Primary antibodies were diluted in blocking buffer and applied at 4 °C overnight. Secondary antibodies were applied for 2 h at room temperature. Nuclei were stained with DAPI. Antibodies used are listed in Table 3. Cells were examined using the Olympus BX60 fluorescence microscope and imaged using Olympus DP-Controller 3.1.1.267 acquisition software (Olympus Corporation, Tokyo, Japan).

Digital karyotyping

Digital karyotyping was performed on LEIi008-A (passage 4) and LEIi009-A (passage 10) iPSC using the Illumina HumanCoreExome-24 Beadchip SNP array (D'Antonio et al., 2017). DNA was isolated using the FlexiGene DNA kit (QIAGEN). CNV analysis was performed on GenomeStudio 2.0 software using the CNVpartition 2.0 plugin (Illumina). To identify genomic alterations (deletions or duplications over 500 kb), B allele frequencies (Fig. 1C), LogR ratios and CNV values were

Table 3
Reagents details.

Antibodies used for immunocytochemistry/flow-cytometry			
	Antibody	Dilution	Company Cat # and RRID
Pluripotency markers	Mouse anti-OCT4	1:200	StemCell Technologies Cat# 60093, RRID: AB_2561766
	Rabbit anti-NANOG	1:100	Abcam Cat# ab21624, RRID: AB_446437
	Rabbit anti-SOX2	1:200	Thermo Fisher Scientific Cat# 48–1400, RRID:AB_2533841
	Mouse anti-TRA-1-81-AlexaFluor 488	1:100	Stem Cell Technologies Cat# 60065 AD, RRID: AB_1089240
Secondary antibodies	Alexa Fluor 546 Goat Anti-Mouse IgG	1:500	Molecular Probes Cat# A-11003, RRID: AB_141370
	Alexa Fluor 488 Goat Anti-Rabbit IgG	1:500	Molecular Probes Cat# A-11008, RRID: AB_143165

Primers		
	Target	Forward/Reverse primer (5′-3′)
Episomal plasmid detection	Reprogramming Plasmids (95 bp product)	AGGTCCCTCGAAGAGGTTCA/TTCCAACGCGAGAAGGTGTT
Pluripotency markers (qPCR)	*OCT4*	CCTGAAGCAGAAGAGGATCACC/AAAGCGGCAGATGGTCGTTTGG
	NANOG	CTCCAACATCCTGAACCTCAGC/CGTCACACCATTGCTATTCTTCG
	KLF4	CATCTCAAGGCACACCTGCGAA/TCGGTCGCATTTTTGGCACTGG
House-keeping genes (qPCR)	*GAPDH*	GTCTCCTCTGACTTCAACAGCG/ACCACCCTGTTGCTGTAGCCAA
Trilineage markers (qPCR)	*PAX6*	CTGAGGAATCAGAGAAGACAGGC/ATGGAGCCAGATGTGAAGGAGG
	OTX1	CTACCCTGACATCTTCATGCGG/GGAGAGGACTTCTTCTTGGCTG
	DCN	AGAGTACCTGGTGGGCTGG/GTGGGCAGAAGTCACTTGAT
	GATA2	CTGTCTGCAACGCCTGTG/GTTCCGAGTCTGGATCCCTT
	AFP	TGAGCACTGTTGCAGAGGAG/TTGTTTGACAGAGTGTCTTGTTGA
Mutation sequencing	*PRPF31* Intron 11-Intron 12	ACTCTGAGCTCACAGAGCAG/GCCATATACGACGCTCTGCT

plotted against genomic location (Supplementary Fig. S2). This method does not reveal copy number neutral changes such as balanced translocations.

Microsatellite analysis

Analysis of microsatellites was performed using the PowerPlex 16HS system (Promega, performed at the Australian Genome Research Facility). Patient fibroblasts (1093-FB, 1374-FB), LEIi008-A and LEIi009-A were genotyped at the loci D18S51, D21S11, TH01, D3S1358, Penta E, FGA, TPOX, D8S1179, vWA, CSF1PO, D16S539, D7S820, D13S317, D5S818, Penta D and Amelogenin (Supplementary Fig. S1). Results are shown as a heatmap, demonstrating matching genotypes at all loci examined.

Funding

This work was funded by the National Health and Medical Research Council of Australia (grants 1142962 and 1116360), Ophthalmic Research Institute of Australia, Retina Australia and generous donations from the Saleeba, Miocevich and McCusker families.

Appendix A. Supplementary data

Supplementary data to this article can be found online at https://doi.org/10.1016/j.scr.2018.11.018.

References

D'Antonio, M., Woodruff, G., Nathanson, J.L., D'Antonio-Chronowska, A., Arias, A., Matsui, H., Williams, R., Herrera, C., Reyna, S.M., Yeo, G.W., Goldstein, L.S.B., Panopoulos, A.D., Frazer, K.A., 2017. High-throughput and cost-effective characterization of induced pluripotent stem cells. Stem Cell Rep. 8, 1101–1111.

Frio, T. Rio, Wade, N.M., Ransijn, A., Berson, E.L., Beckmann, J.S., Rivolta, C., 2008. Premature termination codons in PRPF31 cause retinitis pigmentosa via haploinsufficiency due to nonsense-mediated mRNA decay. J. Clin. Invest. 118, 1519–1531.

Mellough, C.B., Sernagor, E., Moreno-Gimeno, I., Steel, D.H., Lako, M., 2012. Efficient stage-specific differentiation of human pluripotent stem cells toward retinal photoreceptor cells. Stem Cells (Dayton, Ohio) 30, 673–686.

Rose, A.M., Bhattacharya, S.S., 2016. Variant haploinsufficiency and phenotypic non-penetrance in PRPF31-associated retinitis pigmentosa. Clin. Genet. 90, 118–126.

Wilkie, S.E., Morris, K.J., Bhattacharya, S.S., Warren, M.J., Hunt, D.M., 2006. A study of the nuclear trafficking of the splicing factor protein PRPF31 linked to autosomal dominant retinitis pigmentosa (ADRP). Biochim. Biophys. Acta 1762, 304–311.